

Bias dependence of Schottky barrier height in GaAs from internal photoemission and current-voltage characteristics

Toshiki Ishida and Hideaki Ikoma

Faculty of Science and Technology, Science University of Tokyo, Noda, Chiba 278, Japan

(Received 12 November 1992; accepted for publication 15 June 1993)

Bias dependence of Schottky barrier height ϕ_B was directly measured using an internal photoemission effect in Au-*n*-GaAs Schottky barrier diodes under both the forward and reverse applied voltages. ϕ_B increased by about 0.015–0.016 eV as the forward bias increased from 0 to 0.3 V. This is probably due to an applied-voltage-induced change in electron population in the interface states. The results were compared with the bias dependence derived from dark forward current-voltage (*I*-*V*) characteristics. Both bias dependences were in good agreement, indicating that nonideal forward *I*-*V* characteristics (a deviation from the ideal thermionic emission theory) could be fully explained by the bias dependence of ϕ_B for diodes of a relatively good quality (an ideality factor, $n=1.02$ – 1.07). The effective Richardson constant A^{**} was calculated to be about 1.3 – $1.4 \times 10^5 \text{ A K}^{-2} \text{ m}^{-2}$ for the diodes of the lower n values using the value of the measured Schottky barrier height at zero bias. These values of A^{**} were higher than the calculated value of about $8 \times 10^4 \text{ A K}^{-2} \text{ m}^{-2}$ and that of $0.41 \pm 0.15 \times 10^4 \text{ A K}^{-2} \text{ m}^{-2}$ reported by Missous and Rhoderick [J. Appl. Phys. **69**, 7142 (1991)]. This is probably due to an enhancement of an electron tunneling through the high density interface states in our case. ϕ_B decreased by about 0.05–0.06 eV when the reverse voltage increased from 0 to 3.0 V. An image force lowering effect could not account for this large reverse bias dependence of the barrier height. The nonideal reverse *I*-*V* characteristics could not be interpreted solely by the bias dependence of ϕ_B . This discrepancy was attributed to other leakage current mechanisms.

I. INTRODUCTION

A Schottky barrier height of an ideal metal-semiconductor contact equals the difference between a work function of the metal and an electron affinity of the semiconductor.^{1–12} However, in a real metal-semiconductor contact, the barrier height is severely affected by the presence of electronic states at an interface between the metal and the semiconductor. The most important effect of the interface states on the barrier height is a Fermi level pinning effect.^{7–12} The surface Fermi level is pinned at a certain energy level due to a high density of the interface states so that the Schottky barrier height is nearly independent of the metal work function. This was observed in compound semiconductors^{7–12} such as GaAs and InP. There have been many investigations exploring the mechanism of the Fermi level pinning effect.

The interface states are usually populated with electrons. The population of electrons in the interface states changes with a bias voltage applied to the Schottky diode. Then, the Schottky barrier height varies with the applied voltage, which leads to a deviation of the *I*-*V* characteristics from an ideal one calculated from the thermionic emission theory.^{1–6,13,14} This is another effect of the interface states. In these cases, ideality factors obtained from the forward *I*-*V* characteristics are often observed to change with the applied voltage. Very recently, Maeda *et al.*¹³ proposed a Schottky barrier model in which the barrier height changes with the bias voltage due to the change in population of electrons in the interface states. In their model,¹³ it is assumed that both a deviation of an ideality factor from unity and its variation with applied voltage are as-

cribed to the change in the barrier height with the applied voltage.

It is therefore interesting to investigate behaviors of the Schottky barrier height under the applied bias voltage. The Schottky barrier height is usually obtained from either current-voltage (*I*-*V*) or capacitance-voltage (*C*-*V*) characteristics. However, it is difficult to obtain an accurate value of the barrier height from *I*-*V* characteristics because the values of the Richardson constant of GaAs and InP are still controversial. Further, the bias dependence of the barrier height cannot be generally obtained from both *I*-*V* and capacitance-voltage (*C*-*V*) characteristics without any assumption. An internal photoemission measurement is a very useful direct method for obtaining more accurate value of the Schottky barrier height.^{15–18}

In the present study, internal photoemission measurements were performed for Au-GaAs Schottky diodes under the forward and the reverse bias voltages to investigate the bias voltage dependences of the Schottky barrier height. The Schottky barrier height changed with the bias voltage under both the forward and the reverse voltages. The results for the forward bias were compared with the bias dependence of the barrier height derived from the dark forward *I*-*V* characteristics under an assumption that the deviation of an ideality factor n from unity can solely be ascribed to the bias dependence of the barrier height. Both were in a good agreement for the samples with the ideality factor of about 1.02–1.08.

In Sec. II, experimental procedures are described. Experimental results are presented in Sec. III and an analysis and a discussion of experimental results are given in Sec.

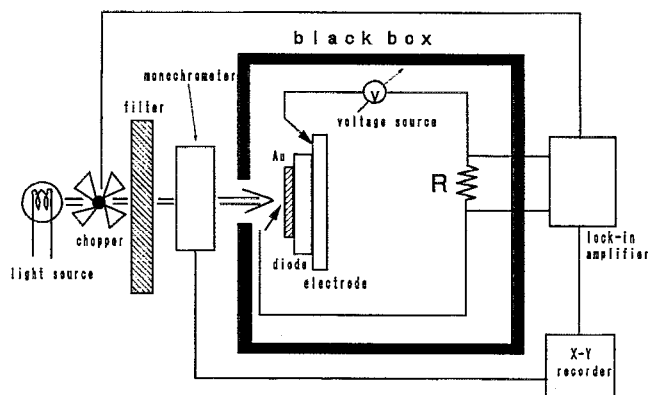


FIG. 1. A block diagram of the experimental setup and a measuring circuit for the internal photoemission measurements.

IV. Finally, a summary and a conclusion are presented in Sec. V.

II. EXPERIMENTAL PROCEDURES

A. Sample preparations

HB (horizontal Bridgman) grown *n*-type GaAs (100) substrates with a free-carrier concentration of about $1 \times 10^{17} \text{ cm}^{-3}$ were employed. The free carrier concentration was estimated from *C-V* measurements at a frequency of 1 MHz. Substrates were cleaned ultrasonically in trichloroethylene, acetone, and deionized water. Substrates were then lightly etched in dilute HCl solution for 5 min to remove native oxides, rinsed in deionized water and blown dry with nitrogen gas. The ohmic contact was formed by evaporating Au-Ge alloy on a back surface of the substrate and annealing at 350 °C for 30 min in a nitrogen ambient. The same organic and the HCl treatments were again carried out to eliminate contaminants and the native oxide on the front surface of the substrate. After being blown dry in nitrogen gas, the substrate was quickly transferred into a vacuum chamber of an evaporator and Au was deposited through a metal mask on it at a vacuum of $(1-2) \times 10^{-6}$ Torr. Very thin semitransparent Au films were formed. Schottky contact size used in the internal photoemission measurements was $1 \times 6 \text{ mm}$.

B. Measurements

Internal photoemission measurements were performed for Au-GaAs Schottky diodes. A block diagram of an experimental setup and a measuring circuit of the internal photoemission is illustrated in Fig. 1. The diode was placed in front of a small slit opened in a black box and the radiation through a monochromator is focused with a lens on a surface of the thin semitransparent Au film on the diode. The radiation from a tungsten lamp was chopped at a frequency of 80 Hz and incident on an entrance slit of the monochromator JASCO CT-25C through a neutral filter. The bias voltage is applied with a conventional dc voltage source as is shown in this figure. The voltage that appeared across a series resistance *R* in the measuring circuit was

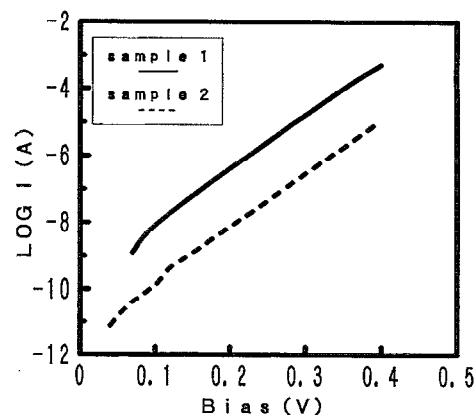


FIG. 2. Forward current-voltage characteristics for the Au-GaAs Schottky diode samples 1 and 2.

amplified with a lock-in amplifier synchronized with the chopping frequency and recorded as a function of an energy $h\nu$ of the incident light on an X-Y recorder. The diode was set on a copper plate to avoid temperature rise due to light illumination together with a use of the neutral filter. The dark *I-V* characteristics of diodes were also measured automatically and continuously with a digital electrometer controlled with a personal computer.

III. EXPERIMENTAL RESULTS

Forward *I-V* characteristics are shown in Fig. 2 for the Au-GaAs Schottky diode samples 1 and 2. The ideality factors (*n*) are about 1.03 and 1.07, respectively, for samples 1 and 2. Sample 1 is considered to be of somewhat better quality than sample 2, because the ideality factor was nearer to unity in sample 1 than in sample 2.

A photoemission yield *Y* was calculated by dividing the measured current through the series resistance *R* by the total number of incident photons. In Figs. 3 and 4, square roots of the photoemission yield \sqrt{Y} (in an arbitrary unit) are plotted as functions of the energy $h\nu$ of the incident

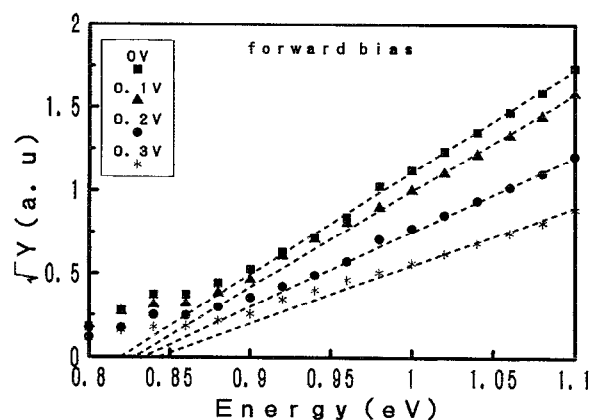


FIG. 3. The square root \sqrt{Y} vs the incident photon energy $h\nu$ under various forward voltages for sample 1.

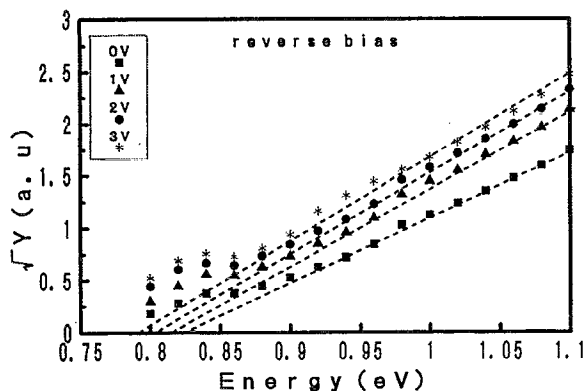


FIG. 4. The square root \sqrt{Y} vs the incident photon energy $h\nu$ under various reverse voltages for sample 1.

light, respectively, under the forward and the reverse bias voltages for sample 1. Values of the forward and the reverse bias voltages are indicated as parameters in both figures.

IV. ANALYSIS AND DISCUSSION OF EXPERIMENTAL RESULTS

A. Analysis of the forward characteristics

The photoemission yield Y is known to be proportional to $(h\nu - \phi_B)^2$, where $h\nu$ is the energy of the incident radiation and ϕ_B is the barrier height measured from the metal Fermi level. Figure 3 shows that the square root \sqrt{Y} of the photoemission yield changes linearly with the incident photon energy $h\nu$ in a range of $h\nu$ between 0.9 and 1.1 eV. The barrier height ϕ_B was obtained as a function of the forward bias voltage V from an extrapolation of this portion of the \sqrt{Y} vs $h\nu$ curve to an energy axis ($\sqrt{Y}=0$). The forward bias dependences of the barrier height ϕ_B thus obtained are exhibited in Figs. 5 and 6, respectively, for samples 1 and 2. The obtained ϕ_B values are shown with closed triangles in both figures. The experimental error

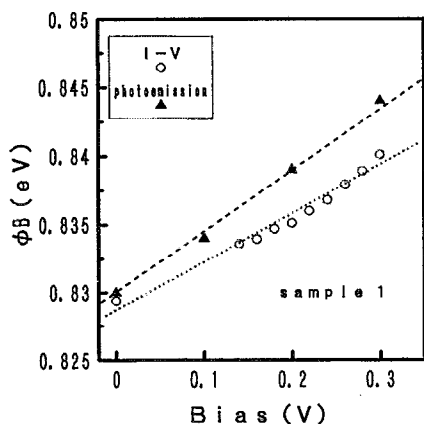


FIG. 5. The forward bias dependence of the Schottky barrier height ϕ_B for sample 1. Closed triangles represent the data obtained from the internal photoemission measurement and closed circles represent the data obtained from the I - V characteristics. Agreement between them is good.

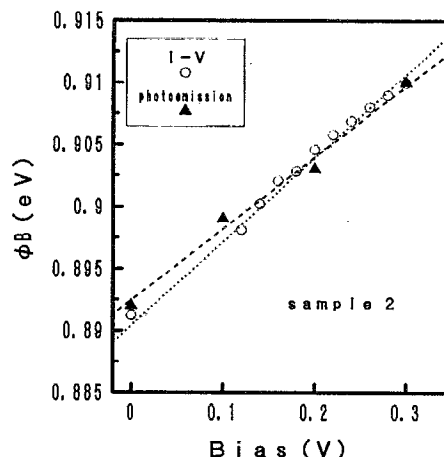


FIG. 6. The forward bias dependence of the Schottky barrier height ϕ_B for sample 2. Closed triangles represent the data obtained from the internal photoemission measurement and closed circles represent the data obtained from the I - V characteristics. Agreement between both is very good.

bars are also indicated in these figures. It can be seen that ϕ_B changes by about 0.015 to 0.016 eV as the forward bias increases from 0 to 0.3 V. The variation $\Delta\phi_B (= \phi_B - \phi_B^0)$ of the barrier height ϕ_B due to the applied voltage was calculated and plotted for both samples 1 and 2 in Fig. 7. Here, ϕ_B^0 is the barrier height at zero bias voltage. The diode of the better quality (sample 1) shows a smaller variation of $\Delta\phi_B$ with the bias voltage than the diode of the poorer quality (sample 2). This trend was quite reproducible.

Using the value of ϕ_B^0 obtained above, an effective Richardson constant A^{**} was derived for each sample. A^{**} probably includes the effect of an electron tunneling through the native oxide inevitably formed between the metal and the semiconductor substrate so that it may be

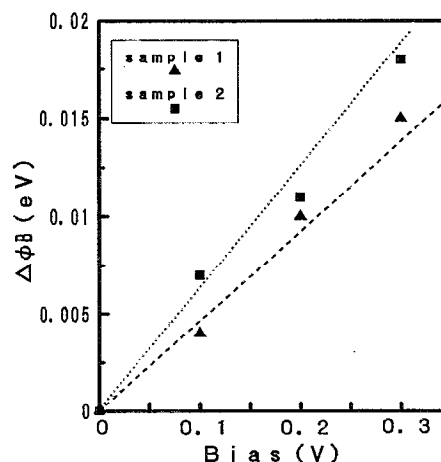


FIG. 7. The variation $\Delta\phi_B$ of ϕ_B from that at zero bias voltage vs the applied bias voltage obtained from internal photoemission measurements for samples 1 and 2.

different for different samples. The effective Richardson constant A^{**} was calculated from the relation,

$$A^{**} = \frac{I_0}{ST} \exp\left(\frac{q\phi_B^0}{kT}\right), \quad (1)$$

where I_0 was obtained by extrapolating the linear part of the $\log I$ vs V curve to $V=0$ as is usual, S is the area of diode, q is the electronic charge, k is the Boltzmann constant, and T is the absolute temperature. Values of A^{**} were about, 1.41×10^5 and $5.69 \times 10^4 \text{ A K}^{-2} \text{ m}^{-2}$, respectively, for samples 1 and 2. For other Au-GaAs diode samples with the ideality factor of 1.02–1.04, the nearly same value of A^{**} was obtained. The former value is somewhat higher than the theoretical value of $8 \times 10^4 \text{ A K}^{-2} \text{ m}^{-2}$, which is usually employed and much higher than that ($=0.41 \pm 0.15 \times 10^4 \text{ A K}^{-2} \text{ m}^{-2}$) reported by Missous and Rhoderick.¹⁹ In the work of Missous and Rhoderick,¹⁹ the Schottky diodes were fabricated using a molecular-beam epitaxy in an ultrahigh vacuum. Therefore, there were no oxides of GaAs between the metal and the GaAs substrate. In our samples, on the other hand, the native oxides were grown during the sample preparation. Hence, there was a high density of the interface states between the native oxide and the GaAs substrate. The interface states assist a tunneling of electrons from the semiconductor to the metal. Therefore, the existence of the high density of the interface states probably enhances the tunneling probability of electrons from the semiconductor to the metal through the interface states. This probably is the reason that the high values of the effective Richardson constant, much above its theoretical value and that obtained by Missous and Rhoderick,¹⁹ is obtained.

Previously, Rhoderick¹ pointed out that the ideality factor n is higher than about 1.02–1.03 even in the ideal GaAs diode due to the contribution from the field emission effect to I - V characteristics. However, Missous and Rhoderick¹⁹ reported the ideality factor n of less than 1.01 at room temperature and about 1.002 at 402 K for Al-GaAs Schottky barrier diodes fabricated in an ultrahigh vacuum. Then, the ideality factor is considered to really approach unity in an ideal limit in GaAs. In order to compare with photoemission results, the dependence of the barrier height ϕ_B on the bias voltage V was derived from an analysis of the dark forward I - V characteristics assuming that both the deviation of the ideality factor from unity and its variation with the bias voltage can be fully attributed to the bias dependence of the Schottky barrier height. The method of analysis used here is schematically shown in Fig. 8. A solid line exhibits the real I - V relation measured and two broken lines A and B are ideal I - V characteristics with the ideality factor of unity ($n=1$) and different barrier heights. The barrier height $\phi_B(V_1)$ at a bias voltage V_1 is assumed to be equal to that of the ideal I - V characteristics represented by the broken line A which crosses the real I - V curve at a point (V_1, I_1) . For different voltage (for example, V_2), the broken line A is moved parallel to the line B as is shown in the figure. The bias dependence of the barrier height was thus obtained from the I - V characteristics.

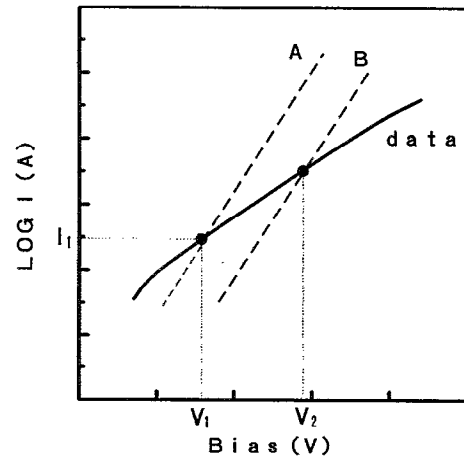


FIG. 8. A schematic representation of the analysis used here to derive the bias dependence of ϕ_B from the I - V characteristics. A solid line represents the actually observed I - V characteristics and two broken lines A and B are ideal ones ($n=1$) with different barrier heights.

In calculation of ϕ_B , the Richardson constant A^{**} obtained above was used for each sample.

The bias dependences of the barrier height ϕ_B thus derived from the I - V characteristics are exhibited in Figs. 5 and 6 with open circles for samples 1 and 2, respectively. The bias dependence of ϕ_B obtained from the I - V characteristics is in good agreement with that observed directly from the internal photoemission experiments for both samples. This indicates that the nonideal forward I - V characteristics (the deviation of n from unity and the bias dependence of n) can fully be explained by the change of the barrier height with the bias voltage possibly, due to the carrier population change in the interface states for these samples.

To see the bias dependence of the ideality factor n for these samples, n was calculated from the experimental forward I - V characteristics using the following equation:

$$n = \frac{qV}{kT} \ln \left[\frac{I}{SA^{**}T} \exp\left(\frac{q\phi_B}{kT}\right) + 1 \right]. \quad (2)$$

Here, I and V are the observed values of the current and the voltage. ϕ_B obtained from internal photoemission experiments and A^{**} determined above are employed. In Fig. 9, n is plotted as a function of the bias voltage V for samples 1 and 2. n slightly decreases in sample 1, whereas it increases with the bias voltage in sample 2. However, the change in n with the bias voltage is very small in these samples.

B. Analysis of the reverse characteristics

The bias voltage dependence of the Schottky barrier height ϕ_B was derived under the reverse bias condition similarly with the forward bias case. Figure 4 shows that \sqrt{Y} changes linearly with $h\nu$ in a range of $h\nu$ between about 0.9 eV and about 1.1 eV. ϕ_B was thus obtained by extrapolating the linear portion of \sqrt{Y} vs the $h\nu$ curve to an energy axis ($\sqrt{Y} = 0$) in Fig. 4. The bias dependences of

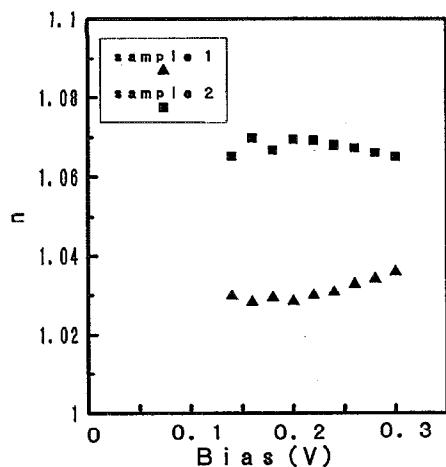


FIG. 9. The ideality factor n as a function of the forward bias voltage obtained from Eq. (2) for sample 1.

$\Delta\phi_B$ are shown in Fig. 10 for samples 1 (closed circles) and 2 (open circles), where $\Delta\phi_B(=\phi_B-\phi_B^0)$ is the change in ϕ_B due to the applied voltage. This figure shows that the barrier height decreases with an increase in the reverse bias voltage, which is consistent with the data reported by Parker *et al.*¹⁷ It changes by about 0.05–0.06 eV as the reverse voltage increases from 0 to 3.0 V. $\Delta\phi_B$ is again smaller in the better quality sample 1 than in the poorer quality sample 2. A solid line in Fig. 10 represents calculated changes $\Delta\phi_{BI}$ of the barrier height due to an image force lowering effect. $\Delta\phi_{BI}$ was obtained from the following equation:^{1,16}

$$\Delta\phi_{BI} = \frac{q^3 N_D (V + V_D - kT/q)}{8\pi^2 \epsilon_0^3 \epsilon_s^2 \epsilon_d}, \quad (3)$$

where q is the electronic charge, N_D is the donor concentration, V is the applied voltage, T is the absolute temperature, k is the Boltzmann constant, ϵ_0 is the dielectric constant of a vacuum, ϵ_s is the relative dielectric constant of GaAs, and V_D is a diffusion potential. ϵ_d is an image force dielectric constant. If an electron transit time through the depletion layer of the semiconductor ϵ_d is shorter than the dielectric relaxation time, ϵ_d is expected to be smaller than the static dielectric constant ϵ_s . However, it has been known¹ that this image force dielectric constants of Si, Ge, and GaAs are approximately the same as the corresponding static values. Then, ϵ_d is here set equal to ϵ_s : $\epsilon_d = \epsilon_s = 11.5$ (the value for GaAs bulk crystal). As for the value of V_D , the experimentally obtained one from C - V characteristics was employed. In Fig. 10, $\Delta\phi_{BI}$ is shown to be much smaller than the observed $\Delta\phi_B$. Hence, the image force lowering effect cannot solely explain the change in the barrier height with the reverse bias voltage. This is also in accord with the data of Parker *et al.*¹⁷ The difference between the observed $\Delta\phi_B$ and $\Delta\phi_{BI}$ is considered to be attributed to the effect of the interface states.

In order to know correlations of the observed bias dependence of $\Delta\phi_B$ to the reverse I - V characteristics, the I - V

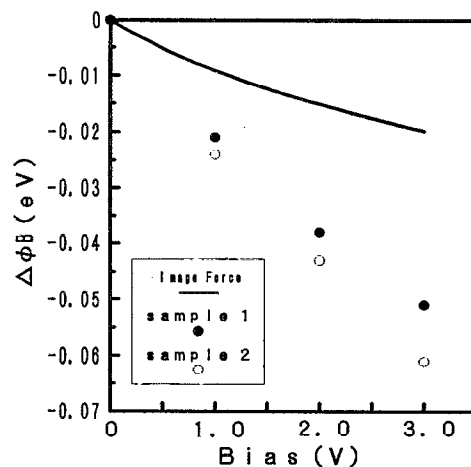


FIG. 10. The variation $\Delta\phi_B$ of ϕ_B from that at zero bias vs the reverse bias voltage obtained from the internal photoemission measurement for samples 1 (closed circles) and 2 (open circles). A dotted line represents the bias dependence of $\Delta\phi_{BI}$ due to the image lowering effect.

characteristics was calculated on a basis of the interfacial layer model proposed by Maeda *et al.*¹³ According to this model, the reverse current I can be calculated by¹³

$$I = \frac{kT\sigma_0}{q} \exp\left(\frac{q\Delta\phi_B}{kT}\right), \quad (4)$$

where, $\sigma_0 = (V/I)_{V=0}$, an extrapolated value of a conductance to $V=0$. The bias dependence of ϕ_B obtained above was used to calculate I . The calculated reverse I - V characteristics are shown in Fig. 11 with closed circles. A solid line represents the dark reverse I - V characteristics observed and a dotted line ideal saturation currents for sample 1. The change in ϕ_B with the bias voltage cannot fully explain the nonideal reverse I - V characteristics. The discrepancy between those is probably attributed to some

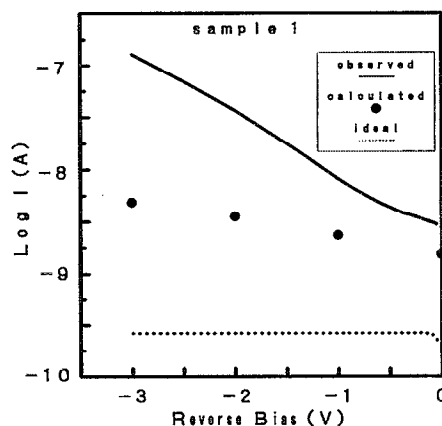


FIG. 11. Reverse current-voltage characteristics for sample 1. Solid line is the observed I - V curve. Closed circles corresponds to that calculated using the interfacial layer model proposed by Maeda *et al.* (Ref. 13) and the experimentally obtained change in ϕ_B with the bias voltage. A dotted line represents the ideal saturation current.

leakage currents due, for example, to the generation-recombination mechanism, the edge leakage and so on.

V. SUMMARY AND CONCLUSIONS

Internal photoemission measurements were performed on Au-GaAs Schottky diodes under the forward and the reverse voltage to investigate the bias voltage dependence of the Schottky barrier height ϕ_B . Ideality factors n of samples used were about 1.02–1.07. ϕ_B was found to increase with the forward bias voltage V . It increased by 0.015–0.016 eV as V was increased from 0 to 0.3 V. The bias dependence of $\Delta\phi_B$ was smaller for the better (lower n) sample than for the poorer (higher n) sample. This bias dependence of $\Delta\phi_B$ is probably attributed to the electron population change in the interface states with the applied voltage. The effective Richardson constant A^{**} was calculated using the above observed value of ϕ_B^0 (the barrier height at zero bias voltage) to be about $1.3\text{--}1.4 \times 10^5 \text{ A K}^{-2} \text{ m}^{-2}$ for better samples ($n=1.02\text{--}1.04$) and $5.6 \times 10^4 \text{ A K}^{-2} \text{ m}^{-2}$ for the poorer sample ($n=1.07$). A^{**} includes the effect of electron tunneling through the native oxide and may be different for the different samples. The forward I - V characteristics were analyzed to deduce the bias dependence of ϕ_B provided that the nonideality (the deviation of the ideality factor n from unity and its variation with the bias) of the forward I - V characteristics can be fully attributed to the bias (V) dependence of ϕ_B . The ϕ_B vs V relation thus obtained was in a good agreement with those observed in internal photoemission experiments. This supports that the nonideal forward I - V characteristics (the deviation of the ideality factor from unity and its bias variation, if any) can be fully attributed to the bias dependence of the Schottky barrier height due to the electron population change in the interface states.

Under the reverse voltage condition, ϕ_B was observed to decrease with an increase in the voltage V . ϕ_B changed by about 0.05–0.06 eV when the reverse voltage was increased from 0 to 3.0 V. The bias dependence was again smaller in the lower n sample. The observed change in $\Delta\phi_B$

with the bias was much higher than that due to the image force lowering. The difference between them is probably attributed to the effect of the interface states.

The reverse I - V characteristics were calculated on a basis of the recently proposed interfacial layer model by Maeda *et al.*¹³ and using the above obtained bias dependencies of ϕ_B . The observed reverse current was much higher than the calculated one. The discrepancy is ascribed to some other leakage current mechanisms.

ACKNOWLEDGMENTS

The authors are indebted to Professor K. Maeda and Dr. I. Umezu of the Faculty of Industrial Science and Technology, Science University of Tokyo for providing the measuring apparatus of internal photoemission and very fruitful discussions.

¹E. H. Rhoderick, *Metal-Semiconductor Contacts* (Clarendon, Oxford, 1978).

²A. M. Cowley and S. M. Sze, *J. Appl. Phys.* **36**, 3212 (1965).

³C. R. Crowell, H. B. Shore, and E. E. LaBate, *J. Appl. Phys.* **36**, 3843 (1965).

⁴C. R. Crowell and S. M. Sze, *Solid State Electron.* **9**, 1035 (1971).

⁵H. C. Card and E. H. Rhoderick, *J. Phys. D* **4**, 1589 (1971).

⁶J. D. Levine, *J. Appl. Phys.* **42**, 3991 (1971).

⁷W. E. Spicer, P. W. Chye, P. R. Skeath, C. Y. Su, and I. Lindau, *J. Vac. Sci. Technol.* **16**, 1422 (1979).

⁸E. Ikeda, H. Hasegawa, S. Ohtsuka, and H. Ohno, *Jpn. J. Appl. Phys.* **27**, 180 (1988).

⁹W. E. Spicer, N. Newman, C. J. Spindt, Z. Liliental-Weber, and E. R. Weber, *J. Vac. Sci. Technol. A* **8**, 2084 (1990).

¹⁰J. Tersoff, *Surf. Sci.* **168**, 275 (1986).

¹¹H. Hasegawa and H. Ohno, *J. Vac. Sci. Technol. B* **4**, 1130 (1986).

¹²H. Hasegawa, Li He, H. Ohno, T. Sawada, T. Haga, Y. Abe, and H. Takahashi, *J. Vac. Sci. Technol. B* **5**, 1097 (1987).

¹³K. Maeda, I. Umezu, H. Ikoma, and T. Yoshimura, *J. Appl. Phys.* **68**, 2858 (1990).

¹⁴H. Ikoma and K. Maeda, *Jpn. J. Appl. Phys.* **30**, 19 (1991).

¹⁵C. R. Crowell, W. G. Spitzer, L. E. Howarth, and E. E. LaBate, *Phys. Rev.* **127**, 2006 (1962).

¹⁶S. M. Sze, C. R. Crowell, and D. Kahn, *J. Appl. Phys.* **35**, 2534 (1964).

¹⁷G. H. Parker, T. C. McGill, C. A. Mead, and D. Hoffman, *Solid State Electron.* **11**, 201 (1968).

¹⁸S. M. Sze, *Physics of Semiconductor Devices* (Wiley, New York, 1981).

¹⁹M. Missous and E. H. Rhoderick, *J. Appl. Phys.* **69**, 7142 (1991).